100-photon microwave ionization of Rydberg atoms in a static electric field

Giuliano Benenti,[1,2,3] Giulio Casati,[1,2,3] and Dima L. Shepelyansky[4,*]
[1]*International Centre for the Study of Dynamical Systems, Via Lucini 3, 22100 Como, Italy*
[2]*Istituto Nazionale di Fisica della Materia, Unità di Milano, Via Celoria 16, 20133 Milano, Italy*
[3]*Istituto Nazionale di Fisica Nucleare, Sezione di Milano, Via Celoria 16, 20133 Milano, Italy*
[4]*Laboratoire de Physique Quantique, UMR C5626 du CNRS, Université Paul Sabatier, F-31062 Toulouse, France*
(Received 23 October 1997)

We present analytical and numerical results for the microwave excitation of nonhydrogenic atoms in a static electric field when up to 1000 photons are required to ionize an atom. For small microwave fields, dynamical localization in photon number leads to exponentially small ionization while above quantum delocalization border ionization goes in a diffusive way. For alkali-metal atoms in a static field the ionization border is much lower than in hydrogen due to internal chaos.
[S1050-2947(98)02203-3]

PACS number(s): 32.80.Rm, 05.45.+b, 72.15.Rn

After two decades of investigations initiated by the pioneering experiment of Bayfield and Koch in 1974 [1], the main features of the microwave ionization of highly excited hydrogen atoms are well understood [2–4]. Generally, this ionization takes place due to the emergence of chaos in the corresponding classical problem, above a certain microwave intensity threshold. In the chaotic regime, quantum excitation proceeds via a diffusive absorption and reemission of field photons, which eventually leads to ionization. For a real atom the quantum process can be either close to the classical diffusion, or strongly suppressed when the field ϵ is below a quantum delocalization border $\tilde{\epsilon}_q$. This suppression is due to the dynamical localization of classical chaos which is produced by quantum interference. In the localized case the distribution over the levels drops exponentially with the photon number. This dynamical localization is analogous to the Anderson localization in quasi-one-dimensional disordered solids, with the photon number playing the role of lattice index. The quantum delocalization takes place if the localization length $\ell_\phi > N_I$, where, in atomic units, $N_I = 1/(2n_0^2\omega)$ is the number of photons required for ionization, with n_0 being the initial principal quantum number and ω the field frequency.

An absolutely different scenario for the microwave ionization of alkali-metal Rydberg atoms was proposed by Gallagher and co-workers based on experimental results in the regime with small rescaled frequency $\omega_0 = \omega n_0^3 \ll 1$ [5,6]. According to this scenario, ionization appears due to a chain of consecutive Landau-Zener transitions between nearby levels, which eventually brings the electron into the continuum. These transitions take place between the eigenstates on an instantaneous basis for Rydberg atom in a static electric field. In the presence of quantum defects the Stark manifolds exhibit a structure of avoided crossings only for sufficiently strong fields with $\epsilon > 1/n_0^5$. Indeed, the experiments [5,6] were in agreement with the $\epsilon \sim 1/n_0^5$ dependence for the microwave ionization threshold, and not with the static field border $\epsilon_s = 1/(9n_0^4)$. This was considered experimental confirmation of the above scenario. However, this picture does not explain in fact how the propagation actually occurs via the chain of these transitions, and why the overlapping of two nearby levels guarantees that the electron will pass through the whole chain. The comparison between the thresholds for hydrogen [4] and for alkali-metal atoms [5–7] clearly shows that the border is lower in the latter case, and that therefore it is related to the quantum defects δ_l of alkali atoms. Since these defects are different from zero only for orbital momentum $l < 3$, the situation is purely quantum, and cannot be treated by the quasiclassical approach used for the hydrogen atom [2]. This is the reason why so long after the experiments were performed [5,6], no detailed theory has been developed. To demonstrate the theoretical difficulty, we note that hundreds of photons are required to ionize atoms in this regime ($N_I = n_0/2\omega_0 = 300$ for $n_0 = 60$ and $\omega_0 = 0.1$).

In this paper we propose another mechanism for the microwave ionization of Rydberg atoms in a static electric field that is qualitatively different from the scenario of Gallagher and co-workers. We argue that ionization in this case is not due to Landau-Zener transitions but due to a quantum diffusive excitation in energy E (or in the photon number $N = E/\omega$). Such quantum diffusion in the low-frequency regime $1/n_0 < \omega_0 \ll 1$ becomes possible due to the appearance of quantum chaos for Rydberg atoms in a static electric field. Indeed, a recent theoretical study [8] showed that the level spacing statistics $P(s)$ in such atoms, for a sufficiently strong static field, is described by the random matrix theory (RMT). These results also indicate a chaotic structure of eigenstates. This internal quantum chaos can lead to a diffusive excitation in energy even for a quite weak microwave field. In this respect, the situation is different from the hydrogen atom, where chaos appears only above some classical field threshold. Another consequence of internal chaos is an increase in the density of effectively coupled states ρ_c. This gives a larger localization length ℓ_q ($\ell_q \propto \rho_c$) and therefore

*Also at Budker Institute of Nuclear Physics, 630090 Novosibirsk, Russia.

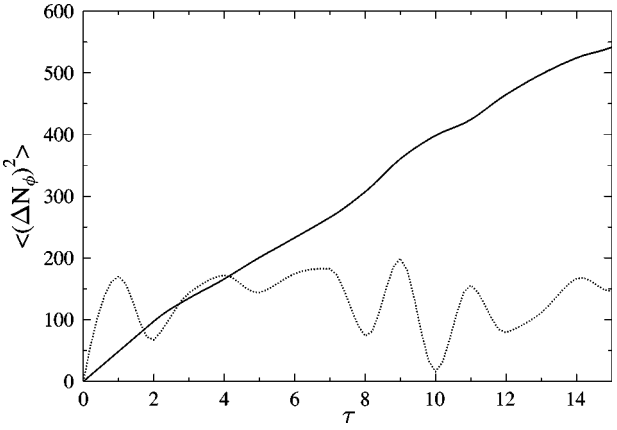

FIG. 1. Photon number square variance $\langle(\Delta N_\phi)^2\rangle$ vs number of microwave periods τ at $n_0=60$, $\epsilon_{s0}=0.02$, $\epsilon_0=0.03$, and $\omega_0=0.1$: diffusive excitation for Rb (full curve $D_q/D_0=0.005$), and small oscillations for hydrogen (dotted curve with 100 times magnification).

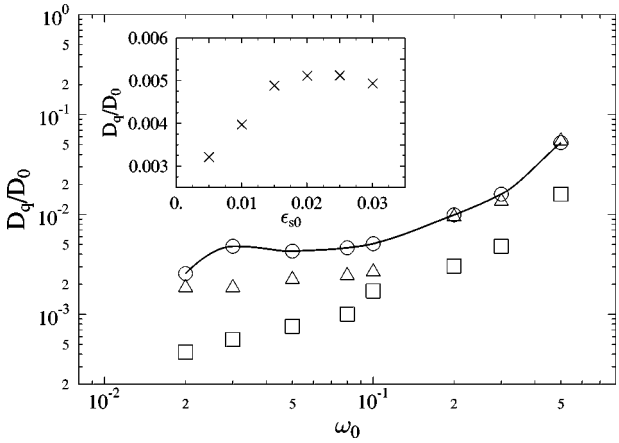

FIG. 2. Diffusion rate ratio D_q/D_0 as a function of microwave frequency ω_0 for Rb (circles), Na (triangles), and Li (squares) at $n_0=60$ and $\epsilon_{s0}=0.02$. The full line is drawn to guide the eye. The inset illustrates the weak dependence of D_q/D_0 on ϵ_{s0} for Rb at $\omega_0=0.1$, $0.015\leqslant\epsilon_0\leqslant0.03$ (crosses).

significantly decreases the delocalization border as compared to the hydrogenic case. A similar effect of chaotic enhancement of the localization length due to internal chaos was studied recently for hydrogen atoms in magnetic and microwave fields [9,10].

To check the above picture of quantum photonic diffusion, we numerically studied the excitation of alkali Rydberg atoms (Rb, Na, Li) in a static electric field ϵ_s, and parallel, linearly polarized, microwave field $\epsilon\sin\omega t$, for magnetic quantum number $m=0$. We chose the rescaled value $\epsilon_{s0}=\epsilon_s n_0^4\approx0.02$ so that the statistics $P(s)$ for levels with $55\leqslant n_0\leqslant72$ in Rb and Na was close to the RMT results. At the same time $P(s)$ for Li was closer to Poisson statistics due to a smaller value of quantum defects [11]. Eigenvalues and eigenstates of alkali-metal atoms in a static electric field were obtained by diagonalization of the Hamiltonian on a spherical hydrogenic basis. We used hydrogen dipole matrix elements and introduced the relevant quantum defects taken from Ref. [12] for angular momentum $l<3$ in the alkali-metal energy levels $E_{nl}=-1/[2(n-\delta_l)^2]$. Such an approach is reasonable for Rydberg states since, far from the nucleus, the electron experiences a nearly Coulomb potential. Also, below the saddle point $\epsilon_s n^4=\frac{1}{9}$, only bound states should be included in the basis set. In such a way the eigenvalues were determined with precision better than five digits. The investigation of time evolution is done on the above eigenbasis of an unperturbed problem with $\epsilon=0$. We directly followed the evolution of probability amplitudes in this basis produced by microwave perturbation with dipole matrix elements of z computed on the eigenbasis of an unperturbed problem at $\epsilon=0$. The time integration was done in the same way as in Ref. [2]. The total size of the Hilbert space was usually $M=1150$. The time dynamics showed that an initial eigenstate with energy E_0 spreads diffusively over the unperturbed energies E_λ; that is, the square variance of the photon number $\sigma=\langle(\Delta N_\phi)^2\rangle=\langle(E_\lambda-E_0)^2\rangle/\omega^2$ initially grows linearly with the number of microwave periods τ (see Fig. 1). Our quantum simulation allows us to determine the value of the quantum diffusion rate in energy per unit time $D_q=\langle(\Delta E)^2\rangle/\Delta t$. This rate D_q can be compared with the diffusion rate in hydrogen at $\omega_0=1$, given by $D_0=\epsilon^2 n_0/2$ [2].

The dependence of the ratio D_q/D_0 on the frequency ω_0, for rescaled fields $0.005\leqslant\epsilon_0\leqslant0.03$ ($\epsilon_0=\epsilon n_0^4$), is shown in Fig. 2.

In our computations we consider the most interesting frequency region $\omega_0\leqslant0.5$, where ionization in hydrogen is close to the static field ionization. In our opinion the ratio D_q/D_0 in Fig. 2 is small because collisions with the core, which are responsible for diffusion, happen rarely, with a frequency of classical precession in l, which is $\omega_{s0}=3\epsilon_{s0}\ll1$. Instead, for $\omega_0>1$ the ratio $D_q/D_0\approx1/3\omega_0^{4/3}$ is similar to the hydrogen case [11]. Notice that the dependence of D_q/D_0 on ω_0 is very flat in the interval $0.02<\omega_0<0.3$. The origin of this fact is not quite clear since asymptotically, for small ω_0, one should expect $D_q\propto\omega_0^2$ [9,10]. Apparently, this plateau in frequency appears due to one-photon transitions between levels in the Stark multiplet. As a result its rescaled size is expected to be $\omega_{s0}\approx3\epsilon_{s0}$, which is in approximate agreement with the data of Fig. 2. We also checked that a change of n_0 from 60 to 28 at the same classically scaled parameters $(\epsilon_0,\epsilon_{s0},\omega_0)$ did not affect the ratio D_q/D_0. For small static fields the diffusion rate D_q starts to drop (see the inset in Fig. 2) since the system becomes close to the integrable case at zero static field.

The above diffusive excitation in energy induced by internal chaos may eventually be localized at long times due to quantum interference effects in a way similar to photonic localization in a complex molecular spectrum [13,2]. The localization length ℓ_q, expressed in the number of photons, is proportional to the one-photon transition rate Γ and to the density of coupled states ρ_c: $\ell_q\sim\Gamma\rho_c$ [13]. Since $\Gamma\sim D_q/\omega^2$, we obtain

$$\ell_q=\ell_\phi\frac{D_q}{D_0\omega_0^2}n_0. \tag{1}$$

Here the length ℓ_q is expressed via the localization length in hydrogen $\ell_\phi=3.3\epsilon_0^2 n_0^2$ at $\omega_0=1$. Notice that in the nonhydrogenic case the density of states is, $\rho_c=n_0^4$, due to internal chaos, while in hydrogen the effective density is smaller, that

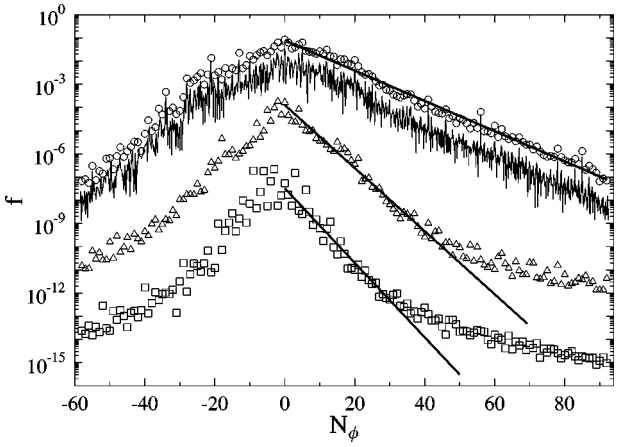

FIG. 3. Probability distribution over the eigenstates at $\epsilon=0$ (full line) and in one-photon intervals (circles) for Rb: $n_0=60, \epsilon_{s0}=0.02, \omega_0=0.1, \epsilon_0=0.005$, $180\leqslant\tau\leqslant200, D_q/D_0=0.0051$, and $\ell_q=9.1$. The straight line shows the fit for exponential localization with $\ell_{qN}=13.3$. The one-photon probabilities are also shown, in the same conditions, for Na (triangles, shifted down by 10^3, $\ell_q=4.8$, and $\ell_{qN}=6.4$) and Li (squares, shifted down by 10^6, $\ell_q=3.1$, and $\ell_{qN}=5.4$).

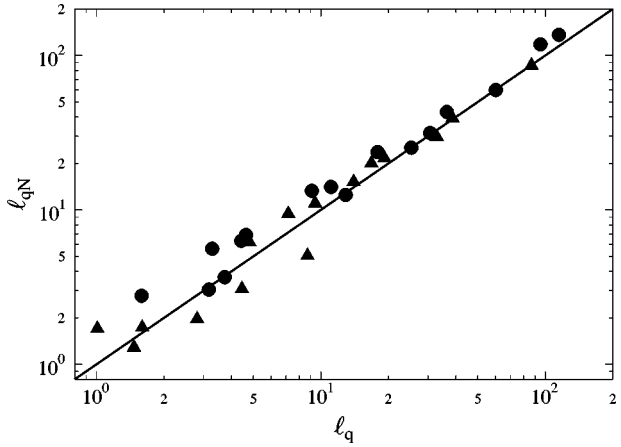

FIG. 4. The numerically computed localization length ℓ_{qN} vs theoretical ℓ_q [Eq. (1)] for Rb (points) and Na (triangles) at $n_0=60, \epsilon_{s0}=0.02$ and $0.02\leqslant\omega_0\leqslant0.5$, $0.003\leqslant\epsilon_0\leqslant0.01$. The straight line gives $\ell_{qN}=\ell_q$, while the numerical average is $\langle\ell_{qN}/\ell_q\rangle=1.17\pm0.28$.

is, $\rho_c=n_0^3$, due to existence of an additional integral of motion [2]. The above expression for ℓ_q is valid for $\ell_q>1$ and $\omega\rho_c=\omega_0 n_0>1$. The localization leads to an exponential decay of probability distribution $|\psi_N|^2\sim\exp(-2|N_\phi|/\ell_q)$ in the photon number $N_\phi=(E_\lambda-E_0)/\omega$.

In order to check the theoretical prediction (1) we numerically computed the quantum evolution following it up to 200 microwave periods. The probability distribution f_λ over the eigenstates of the static field problem ($\epsilon=0$) with energies E_λ, was averaged over 10–20 periods to suppress the fluctuations. An initial state at $\epsilon_{s0}=0.02$ was chosen as an eigenstate with energy $E_{\lambda_0}\approx E_0=-1/2n_0^2$ and $n_0=60$. The system parameters were varied in the intervals $0.02\leqslant\omega_0\leqslant0.5$, $0.003\leqslant\epsilon_0\leqslant0.03$, and $60\leqslant N_I\leqslant1500$. The total basis included up to $M=1150$ states. From f_λ we also determined the total probabilities $f_N=|\psi_N|^2$ in one-photon intervals $[N_\phi-1/2, N_\phi+1/2]$ around integer values of $N_\phi=E_\lambda/\omega$.

A typical example of stationary distribution f is shown in Fig. 3. It clearly demonstrates the exponential localization of diffusive excitation. Indeed, from the maximum the probability drops exponentially by approximately seven orders of magnitude. One can note that among the three cases shown (Rb, Na, Li) the most localized is the case of Li, for which the quantum defect is minimal, and therefore the internal chaos is the most weak. Notice also that in the case of Na and Li, for $f_N<10^{-7}$, the probability f_N starts to decay in a much slower way with $l_q\approx25$ (Fig. 3). We attribute this effect to a significant modification of the hydrogenic basis on highly excited levels, where a static field becomes quite strong and tunneling effects for the probability decay should be taken into account. The change of the total basis size M from 1150 to 770 gave only a 3% variation of probabilities at the tail with $f_N\approx10^{-8}$. Such a check shows that the change of slope represents a physical effect and is not related to the numerics.

In order to find the localization length ℓ_q, we first compute the probabilities f_N in one-photon intervals around integer values of $N_\phi=E_\lambda/\omega$, and then extract the numerical ℓ_{qN} value from the least-squares fit for $\ln f_N$. The analysis of the numerical data in Fig. 4 shows that the localization length l_{qN} varies by two orders of magnitude, being in agreement with the theoretical prediction (1). The theoretical values ℓ_q were computed via the rates D_q taken from Fig. 2.

Equation (1) allows one to determine the quantum delocalization border above which localization effects become unimportant and ionization goes in a diffusive way. This happens for $\ell_q>N_I$, which gives the quantum delocalization border for the rescaled field $\epsilon_q=\tilde{\epsilon}_q n_0^4$:

$$\epsilon_q=0.39\omega^{1/3}\omega_0^{1/6}\sqrt{D_0/D_q}. \tag{2}$$

Our numerical data indeed show that above this border complete delocalization takes place, contrarily to the case of a hydrogen atom at the same field parameters (Fig. 5). Direct

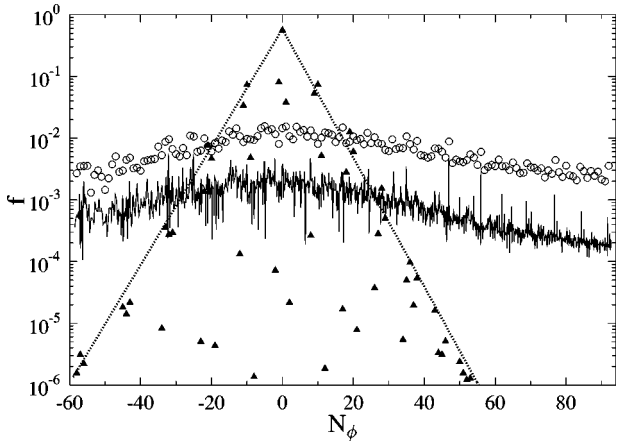

FIG. 5. Same as Fig. 3, but in a delocalized case for Rb, with $\epsilon_0=0.03>\epsilon_q=0.029$ and $40\leqslant\tau\leqslant50$. Full triangles give the one-photon interval probability distribution f_N for a hydrogen atom at the same system parameters (dotted lines show the distribution envelope).

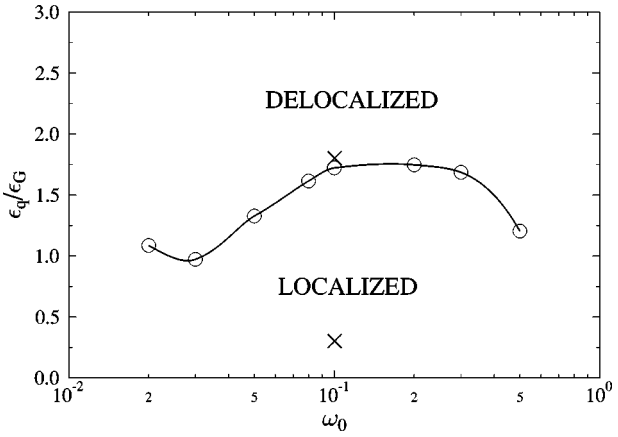

FIG. 6. The ratio of the quantum delocalization border ϵ_q to the border $\epsilon_G = 1/n_0$ vs ω_0 for Rb (circles) obtained from Eq. (2) and data of Fig. 2. The full line is drawn to guide the eye, crosses refer to the cases of Fig. 3 (below) and Fig. 5 (above).

analysis of the probability distribution for the hydrogenic case shows that it is strongly inhomogeneous inside the atomic shells, which leads to strong fluctuations of f_N. We attribute this to the integrability of the hydrogenic atom in weak microwave and static fields.

For fixed ω_0 the delocalization border (2) scales as $\widetilde{\epsilon_q} \sim 1/n_0^5$; that is, it is $\sqrt{n_0}$ times smaller than for hydrogen at $\omega_0 \sim 1$. This drop of ϵ_q is related to the appearance of internal chaos in nonhydrogenic atoms in a static electric field, which effectively enhances the interaction with the microwave radiation. According to Eq. (2) the ratio of ϵ_q to the ionization border proposed by Gallagher and co-workers $\epsilon_G \approx 1/n_0$ depends only on ω_0: $\epsilon_q/\epsilon_G = 0.39\sqrt{\omega_0 D_0/D_q}$. Our data from Fig. 2. indicate that this ratio varies rather weakly with ω_0 in the interval $0.02 < \omega_0 < 0.5$ (see Fig. 6). In spite of the fact that in this range $\epsilon_q \sim \epsilon_G$, the physical interpretation is rather different from the scenario of Gallagher and co-workers. Indeed, the situation for $\epsilon_0 < \epsilon_q \sim 1/n_0$ is strongly nonperturbative, since for $\epsilon_q(2\omega_0/n_0)^{1/2} < \epsilon_0$ many photons are absorbed with $l_q \gg 1$. We also note that even formally the Landau-Zener adiabatic approach cannot be applied to the situation when the frequency is larger than the typical spacing between levels; that is just our case with $\omega_0 n_0 > 1$.

The theory developed above allows one to understand the ionization of atoms in a static electric field. It is possible to expect that for $\omega_0 \ll 1$ the situation will remain similar even without a static field, since its role will be played by a slowly varying microwave field. However, one should be careful in extending the theory to a zero static field case. Indeed, our numerical results show that, in such a case, the probability distribution in the orbital momentum is qualitatively different. For example, at $\epsilon_0 \sim 0.02, \omega_0 \sim 0.2$, only a few l states are mixed, while with additional $\epsilon_{s0} \sim 0.02$ probability spreads over all accessible l. The localization in l space at $\epsilon_{s0} = 0$ was also discussed for Rb atoms in Ref. [14]. The physical reason for this difference is related to the fact that the condition $\omega_0 \ll 1$ is not sufficient to treat the microwave field ϵ_0 as quasistatic. For that, one should require $\omega_0 \ll \omega_{s0} \approx 3\epsilon_0$, since the precession frequency ω_{s0} determines oscillations in l [11]. However, this condition is not compatible with the requirement $\omega_0 > 1/n_0$ for the considered region of n_0. For $\epsilon_{s0} = 0$, chaos is induced by the microwave field, the distribution in l is nonhomogeneous, and a detailed theory for this case becomes more complicated as compared to the nonzero static field where internal chaos is already present.

Another difficulty for direct comparison with the experiments [5,6] is that the latter were mainly done in the regime $\omega_0 < 1/n_0$. There is only one case for Na at $n_0 = 28$, $\omega_0 n_0 = 0.76$, and $\epsilon_{s0} \approx 0.024$ which is not far from our regime [Fig. 2(d) in Ref. [6]]. Here the experiment gives the ionization border $\epsilon_{0ex} \approx 0.002$. This value is about 20 times smaller than the quantum delocalization border given by Eq. (2) with $D_q/D_0 = 0.0027$. We relate this difference to a tunneling ionization in a static field which becomes important for very long interaction times (3×10^5 Kepler periods in Ref. [6]). Indeed, our preliminary numerical data [11] show that there is a change of slope in the probability decay similar to one in Fig. 3 ($l_{qN} \approx 4$ for $f_N > 10^{-5}$ and $l_{qN} \approx 25$ for $f_N < 10^{-5}$). This means that in this case tunneling ionization plays a dominant role, while the microwave only slightly increases its rate. An increase of the principal quantum number up to $n_0 = 60$ strongly suppresses the tunneling in a static field, and the diffusive microwave excitation becomes dominant (Figs. 3 and 5). The effects of tunneling for $n_0 \approx 30$ will become less important for experiments with a shorter interaction time ($\tau \sim 100$), in which the dynamical localization dominates. It is also possible that for such long times as in Ref. [6] some noise in a microwave signal can strongly affect ionization. The above discussion shows that more detailed experimental investigations of microwave ionization in a static electric field are highly desirable. They will allow us to make a detailed test of dynamical localization theory in the regime when up to 1000 photons are required to ionize an atom.

[1] J. E. Bayfield and P. M. Koch, Phys. Rev. Lett. **33**, 258 (1974).
[2] G. Casati, I. Guarneri, and D. L. Shepelyansky, IEEE J. Quantum Electron. **24**, 1420 (1988).
[3] R. V. Jensen, S. M. Susskind, and M. M. Sanders, Phys. Rep. **201**, 1 (1991).
[4] P. M. Koch and K. A. H. van Leeuwen, Phys. Rep. **255**, 290 (1995).
[5] P. Pillet, H. B. van den Heuvell, W. W. Smith, R. Kachru, N. H. Tran, and T. F. Gallagher, Phys. Rev. A **30**, 280 (1984); T. F. Gallagher, C. R. Mahon, P. Pillet, P. Fu, and J. B. Newman, *ibid.* **39**, 4545 (1989).
[6] C. Y. Lee, J. M. Hettema, T. F. Gallagher, and C. W. S. Conover, Phys. Rev. A **46**, 7048 (1992).
[7] M. Arndt, A. Buchleitner, R. N. Mantegna, and H. Walther,

Phys. Rev. Lett. **67**, 2435 (1991).
[8] M. Courtney, H. Jiao, N. Spellmeyer, and D. Kleppner, Phys. Rev. Lett. **73**, 1340 (1994); Phys. Rev. A **51**, 3604 (1995).
[9] F. Benvenuto, G. Casati, and D. L. Shepelyansky, Phys. Rev. A **55**, 1732 (1997).
[10] G. Benenti, G. Casati, and D. L. Shepelyansky, Phys. Rev. A **56**, 3297 (1997).
[11] G. Benenti, G. Casati, and D. L. Shepelyansky (unpublished).
[12] C.-J. Lorenzen and K. Niemax, Phys. Scr. **27**, 300 (1983); T. P. Hezel, C. E. Burkhardt, M. Ciocca, L-W. He, and J. J. Leventhal, Am. J. Phys. **60**, 329 (1992).
[13] D. L. Shepelyansky, Physica D **28**, 103 (1987).
[14] R. Blümel, A. Buchleitner, R. Graham, L. Sirko, U. Smilansky, and H. Walther, Phys. Rev. A **44**, 4521 (1991).